MRI Guided IMRT Commissioning: a Hybrid Approach

H. Harold Li, PhD
Professor of Radiation Oncology
Department of Radiation Oncology
Washington University School of Medicine

Washington University in St. Louis
School of Medicine

Disclosure

Received honoraria and travel reimbursement from ViewRay, Inc.

Washington University School of Medicine in St. Louis — Department of Radiation Oncology, Medical Physics Division

Learning objectives

1) Review MRgIMRT dosimetry challenges
2) Learn a hybrid approach: experimental and computational dosimetry
3) Review future developments

Washington University School of Medicine in St. Louis — Department of Radiation Oncology, Medical Physics Division

January 15, 2014

MRIDIAN-Cobalt system

- 3 Co-60 sources (120 degrees apart)
  - Dose rate: 550-600 cGy/min from all 3
  - 15,000 Ci each (maximum)
- Maximum field size = 27x27 cm^2
- Bore size = 70 cm
- 0.35-Tesla split magnet
  - Strong enough to produce quality images but minimal dosimetric effect of MR field
- Volumetric imaging
  - 20 sec
  - Volumetric images: 1.6x1.6x3 mm^3
  - 50 cm field-of-view
- Cine sagittal imaging
  - 4 frames per second (single plane)
  - 3.5x3.5x7 mm^2

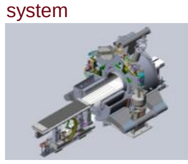

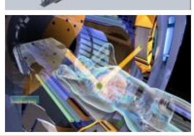

MRIDIAN-Linac system

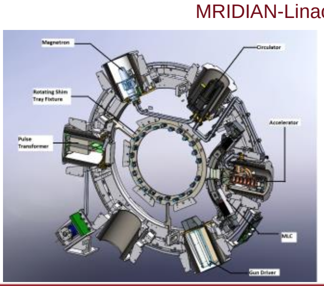

May 14, 2018

Magnetic field affects radiation transport

Dose kernel

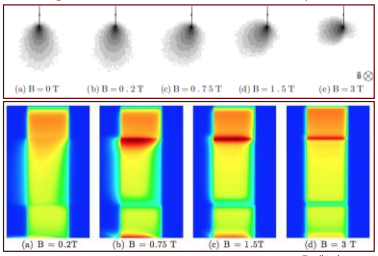

Tissue

Lung

Tissue

Raaijmakers. *et. al.*, PMB 2008

Commissioning an MRgIMRT system is challenging

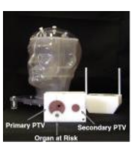

Credentialing results from IMRT irradiations of an anthropomorphic head and neck phantom

Andrea Molineu,[a] Nadia Hernandez, Trang Nguyen, Geoffrey Ibbott, and David Followill
Department of Radiation Physics, The University of Texas MD Anderson Cancer Center, Houston, Texas 77030

Results: The phantom was irradiated 1139 times by 763 institutions from 2001 through 2011. 929 (81.6%) of the irradiations passed the criteria. 156 (13.7%) irradiations failed only the TLD criteria, 21 (1.8%) failed only the film criteria, and 33 (2.9%) failed both sets of criteria. Only 69% of the irradiations passed a narrowed TLD criterion of ±5%.

"Stock" data is not reasonable in every case

Physics Contribution

Treatment Planning System Calculation Errors Are Present in Most Imaging and Radiation Oncology Core-Houston Phantom Failures

James R. Kerns, PhD,[*,†,‡] Francesco Stingo, PhD,[§] David S. Followill, PhD,[*,†,‡] Rebecca M. Howell, PhD,[*,‡] Adam Melancon, PhD,[*] and Stephen F. Kry, PhD[*,†,‡]

[*]Department of Radiation Physics, [†]Imaging and Radiation Oncology Core-Houston, and [§]Department of Biostatistics, The University of Texas MD Anderson Cancer Center; and [‡]Graduate School of Biomedical Sciences, The University of Texas Health Science Center-Houston, Houston, Texas

Received Oct 10, 2016, and in revised form Mar 2, 2017. Accepted for publication Mar 27, 2017.

- IROC-Houston >250 H&N phantom irradiations performed from 2012 to 2016
- Nearly 1 in 5 institutions found to have TPS errors in their IMRT calculations
- Need for careful beam modeling and calculation in the TPS

Relative 3% global dose difference/3 mm DTA gamma metric **NOT** sensitive enough

IMRT commissioning: Multiple institution planning and dosimetry comparisons, a report from AAPM Task Group 119

Gary A. Ezzell
Department of Radiation Oncology, Mayo Clinic Scottsdale, 5777 East Mayo Boulevard, MCSB Concourse, Phoenix, Arizona 89054

Evaluating IMRT and VMAT dose accuracy: Practical examples of failure to detect systematic errors when applying a commonly used metric and action levels

Benjamin E. Nelms, Maria F. Chan, Geneviève Jarry, Matthieu Lemire, John Lowden, Carnell Hampton, and Vladimir Feygelman

Advanced dosimetry methods

Method	Description
Ion chamber	Measure absolute dose in region of interest with micro-chamber (if possible). This method is useful if there is a large enough region of consistent and unidirectional dose bias
Dose profiles	Plot absolute dose profiles, planned vs measured, through region(s) of interest
2%L/2 mm error pattern	Employ a sensitive metric and examine patterns of error in the dose distribution
EPID-based	Use EPID input to predict high-density dose planes for more thorough analysis than sparse arrays. The specific tool used in this study was EPIDose. This implementation of EPID-based dosimetry reconstructs planar dose in a phantom for comparison with TPS-calculated dose, as opposed to comparing EPID images generated by a separate algorithm, which does not audit the TPS dose calculation (Ref. 25)
3D measurement guided dose reconstruction (MGDR)	Use measurement-guided dose reconstruction technique to use QA measurements to estimate 3D dose with the TPS voxel resolution, either on a phantom dose or on the patient CT dataset. The specific tool used in this study was 3DVH
Dose grid inspection	Use graphical tools to inspect the TPS dose grid, including extents, resolution, and volume filled by nonzero dose voxels

Nelms et al. Med Phys 2013

Washington University School of Medicine in St. Louis
Department of Radiation Oncology
Medical Physics Division

Commercially available dosimetry systems

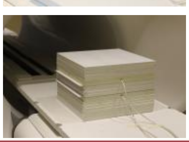

Washington University School of Medicine in St. Louis
Department of Radiation Oncology
Medical Physics Division

3D PRESAGE/ Optical CT dosimetry: Wash U-Duke

On the Need for Comprehensive Validation of Deformable Image Registration, Investigated With a Novel 3-Dimensional Deformable Dosimeter

Titania Juang, BS,[*,†] Shiva Das, PhD,[†] John Adamovics, PhD,[‡] Ron Benning,[‡] and Mark Oldham, PhD[†]

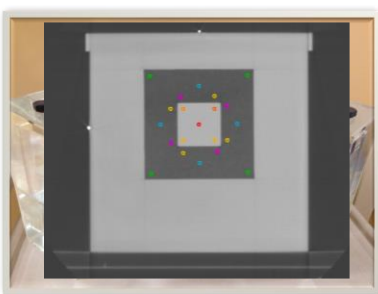

Washington University School of Medicine in St. Louis
Department of Radiation Oncology
Medical Physics Division

Dosimeter response: vertical and lateral shifts

Relative dosimetry with an MR-linac: Response of ion chambers, diamond, and diode detectors for off-axis, depth dose, and output factor measurements

Daniel J. O'Brien[a)]
Department of Radiation Physics, The University of Texas MD Anderson Cancer Center, Houston, TX 77030, USA

the center. The lateral shift of the dose profiles observed with both ionization chambers and solid-state detectors also has implications for the use of ion chamber or diode arrays in QA devices designed for routine or patient-specific QA, as the measured dose distribution may be shifted relative to the true dose distribution. This should be investigated before such a system is used clinically. The use of a shielded diode to

Washington University School of Medicine in St. Louis
Department of Radiation Oncology
Medical Physics Division

Ionization chamber: angular dependence

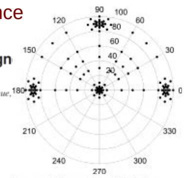

Technical Note: Ion chamber angular dependence in a magn

Michael Reynolds[a)]
Department of Oncology, Medical Physics Division, University of Alberta, 11560 University Avenue, Canada

Results: The Fano test yielded a 0.4% difference between simulation and expected result, which is similar to previous findings and sufficient for the purposes of this study. The angular dose–response map in all cases where the magnetic field is oriented orthogonal to the radiation beam is quite varied and can range from 0.89 to 1.08. Angular deviations as small as 3° can lead to dose–response changes in excess of 1%. When the magnetic field is parallel to the photon beam, the angular dose–response map is homogeneous and less than 1% below 1.0 T.

Ionization chamber: perturbation

Letter to the Editor

Comment on "Testing of the analytical anisotropic algorithm for photon dose calculation" [Med. Phys. 33, 4130–4148 (2006)]

George X. Ding, Dennis M. Duggan, and Charles W. Coffey
Department of Radiation Oncology
Vanderbilt University School of Medicine

(Received 22 February 2007; revised 23 May 2007; accepted for publication 31 May 2007;

Hence, we caution that ionization chambers are not suitable for measuring dose in low-density media where there is a severe perturbation due to electronic disequilibrium. Therefore, conclusion by Van Esch *et al.*[1] regarding AAA accuracy at predicting the dose in inhomogeneities (cork, lung) drawn from RK chamber measurements is inaccurate, especially for small beam field sizes. Our analysis indicates that AAA is accurate for 6 MV (<2%) but is less accurate (>10%) for 18 MV for small fields and in low density media.

EBT3 radiochromic film

Magnetic fields are causing small, but significant changes of the radiochromic EBT3 film response to 6 MV photons

Björn Delfs[1], Andreas A Schoenfeld[1], Daniela Poppinga[1], Ralf-Peter Kapsch[2], Ping Jiang[3], Dietrich Harder[4], Björn Poppe[1] and Hui Khee Looe[1]
[1] University Clinic for Medical Radiation Physics, Medical Campus Pius Hospital, Carl von Ossietzky University, Oldenburg, Germany

The observed small modification of the *OD* versus *D* curve of the radiochromic film EBT3 in the range up to 20 Gy and 1.42 T, hardly exceeding the experimental uncertainty margin, numerically confirms other recent studies on EBT3 film. A stronger magnetic field effect had been observed with the previous product EBT2 exposed to ^{60}Co gamma radiation at 0.35 T.

ArcCHECK-MR diode array

Performance of a cylindrical diode array for use in a 1.5 T MR-linac

A C Houweling[1], J H W de Vries[2], J Wolthaus[2], S Woodings[2], J G M Kok[2], B van Asselen[2], K Smit[2], A Bel[1], J J W Lagendijk[2] and B W Raaymakers[2]

in a transverse 1.5 T magnetic field. To this end, the short-term reproducibility, dose linearity, dose rate dependence, field size dependence, dose per pulse dependence and inter-diode dose response variation of the ArcCHECK-MR diode array were evaluated on a conventional linac and on the MR-linac.

The ArcCHECK-MR diode array performed well for all tests on both linacs, no significant differences in performance characteristics were observed. Differences in the maximum dose deviations between both linacs were less than 1.5%. Therefore, we conclude that the ArcCHECK-MR can be used in a transverse 1.5 T magnetic field.

ArcCHECK-MR diode array: correction factors

An analysis of the ArcCHECK-MR diode array's performance for ViewRay quality assurance

Steven T. Ellefson[1] | Wesley S. Culberson[2] | Bryan P. Bednarz[2] | Larry A. DeWerd[2] | John E. Bayouth[3]

with the ArcCHECK. The current correction factors were applied using both the new and current methods. The new method was also used to apply corrections to the original 19 ViewRay plans. It was found the ArcCHECK systematically reports doses higher than those actually delivered by the ViewRay. Application of the current correction factors by either method did not consistently improve measurement accuracy. As dose deposition and diode response have both been shown to change under the influence of a magnetic field, it can be concluded the current ArcCHECK correction factors are invalid and/or inadequate to correct measurements on the ViewRay system.

Delta4-MR diode array

Characterization of a prototype MR-compatible Delta4 QA system in a 1.5 tesla MR-linac

J H W de Vries[1], E Seravalli[1], A C Houweling[1], S J Woodings[1], R van Rooij[2], J W H Wolthaus[1], J J W Lagendijk[1] and B W Raaymakers[1]

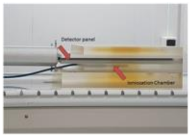

- ❑ Device's feet taken off
- ❑ Adaptations made to the network sockets
- ❑ Power supply cables extended to position the power supply outside of the 5 gauss line

TG-119 results

Structure	Parameter	Goal (Gy)	TG-119 (Gy)	TG-119 St. Dev. (Gy)	^{60}Co (Gy)	^{60}Co / TG-119	^{60}Co /Goal
Head and neck							
PTV	D_{90}	50.00	50.28	0.58	50.98	1.014	1.020
	D_{99}	>46.50	47.04	0.52	46.1	0.980	1.013
	D_{20}	<55.00	52.99	0.93	54.97	1.037	0.999
Cord	Max dose	<40.00	37.41	2.50	39.71	1.061	0.993
Parotid_L	D_{50}	<20.00	17.98	1.84	20.7	1.151	1.035
Parotid_R	D_{50}	<20.00	17.98	1.84	19.92	1.108	0.996
Prostate							
PTV	D_{95}	>75.60	75.66	0.21	75.54	0.998	0.999
	D_5	<83.00	81.43	1.56	82.17	1.009	0.990
Rectum	D_{30}	<70.00	65.36	2.97	64.08	0.980	0.915
	D_{10}	<75.00	73.03	1.50	75	1.027	1.000
Bladder	D_{30}	<70.00	43.94	8.78	46.15	1.050	0.659
	D_{10}	<75.00	62.69	8.15	63.96	1.020	0.853

Test	Location	Meas (Gy)	Plan (Gy)	Meas/plan
AP-PA	Isocenter	1.988	1.990	0.999
Bands	Isocenter	1.422	1.410	1.008
Multi-target	Isocenter	2.085	2.067	1.009
Multi-target	4 cm superior to isocenter	1.062	1.060	1.002
Multi-target	4 cm inferior to isocenter	0.621	0.610	1.018
C-shape	2.5 cm anterior to isocenter	2.152	2.080	1.035
C-shape	1 cm posterior to isocenter	0.917	0.900	1.019
Head & neck	Isocenter	2.215	2.230	0.993
Head & neck	5.5 cm posterior to isocenter	0.917	0.890	1.030
Prostate	Isocenter	1.817	1.830	0.993
Prostate	4.5 cm posterior to isocenter	0.372	0.374	0.995

Wooten et al, Radiother and Oncol 2015

Film measurements: C-Shape

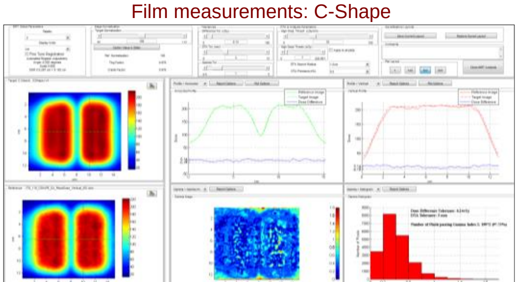

Ionization chamber/HN Box measurement

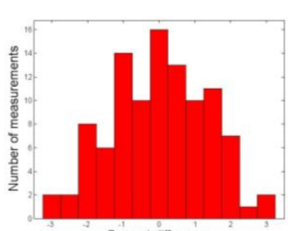

- 102 measurements
- Mean difference: 0.0% ± 1.3%
- Range: -3.0% to 2.9%

Li et al, IJROBP 2015

Radiographic film measurements

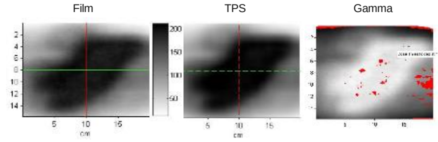

- 30 measurements
- Mean passing rate (relative 3%/3 mm): 94.6% ± 3.4%
- Range: 87.4% to 100%.
- Stacked film measurement provides a much larger sampling of 3D dose distribution than an IC measurement

ArcCHECK-MR measurements

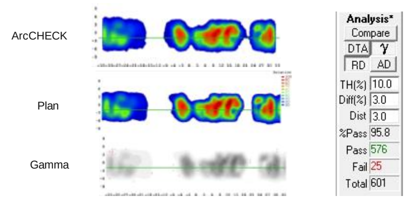

- 34 measurements
- Mean gamma passing rate: 98.9% ± 1.1%

ArcCHECK-MR measurements

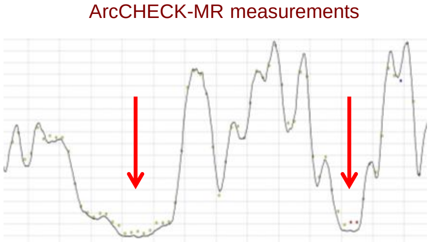

ArcCHECK-MR measurements: MR-LINAC

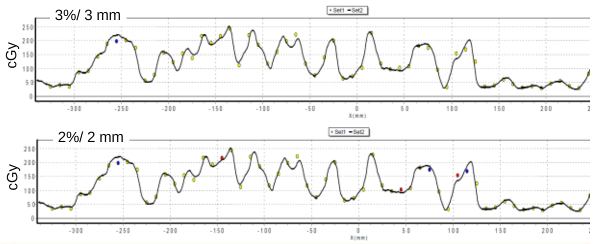

Machine delivery file QA: dynalog

Beam Delivery Verification

Group	#	Plan Beam-Gantry	Beam On Time(s) (Expected/Delivered)	Head	Gantry	Number of Segments	Pass Rate	MLC Error(mm) Mean+/-Std
1	1	3 - 0.0°	54.61 / 54.62	3	0.0°	12 / 12	100 %	-0.0 +/- 0.0
2	2	2 - 255.0°	32.60 / 32.61	2	255.0°	5 / 5	100 %	0.0 +/- 0.0
	3	3 - 15.0°	45.16 / 45.11	3	15.0°	13 / 13	100 %	-0.0 +/- 0.0
3	4	1 - 30.0°	42.18 / 42.18	1	30.0°	8 / 8	100 %	-0.0 +/- 0.0
	5	2 - 150.0°	42.80 / 42.80	2	150.0°	6 / 6	100 %	-0.0 +/- 0.0
	6	3 - 270.0°	18.41 / 18.38	3	270.0°	4 / 4	100 %	-0.0 +/- 0.0
4	7	1 - 45.0°	41.91 / 41.89	1	45.0°	11 / 11	100 %	-0.0 +/- 0.0
	8	2 - 165.0°	28.46 / 28.47	2	165.0°	6 / 6	100 %	-0.0 +/- 0.0
	9	3 - 285.0°	59.67 / 59.69	3	285.0°	8 / 8	100 %	-0.0 +/- 0.0
5	10	1 - 60.0°	51.82 / 51.81	1	60.0°	8 / 8	100 %	-0.0 +/- 0.0
	11	2 - 180.0°	27.39 / 27.39	2	180.0°	8 / 8	100 %	-0.0 +/- 0.0
	12	3 - 300.0°	71.17 / 71.16	3	300.0°	11 / 11	100 %	0.0 +/- 0.0
6	13	1 - 75.0°	51.59 / 51.57	1	75.0°	8 / 8	100 %	-0.0 +/- 0.0
	14	2 - 195.0°	21.75 / 21.75	2	195.0°	6 / 6	100 %	0.0 +/- 0.0
	15	3 - 315.0°	50.79 / 50.73	3	315.0°	10 / 10	100 %	-0.0 +/- 0.0
7	16	1 - 90.0°	72.27 / 72.24	1	90.0°	7 / 7	100 %	-0.0 +/- 0.0
	17	2 - 210.0°	76.17 / 76.16	2	210.0°	11 / 11	100 %	0.0 +/- 0.0
	18	3 - 330.0°	44.06 / 44.05	3	330.0°	11 / 11	100 %	0.0 +/- 0.0
8	19	3 - 345.0°	56.66 / 56.62	3	345.0°	12 / 12	100 %	0.0 +/- 0.0

Beam Fluence Difference

Tolerances

Gantry: 0.5 degree

MLC : 2 mm

Beam-on time: 0.2 sec

2D fluence

Percentage of the pixels with delivery errors less than 2% of the maximum fluence in the field

3D PRESAGE/OCT

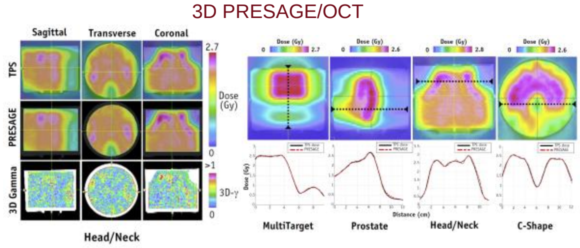

Rankine et al, IJROBP 2017

Electron return effect: single AP field

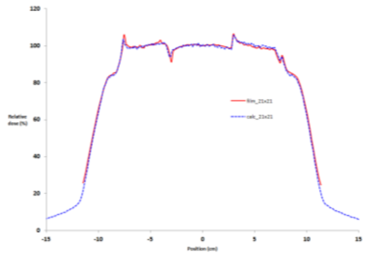

Electron return effect: AP/PA

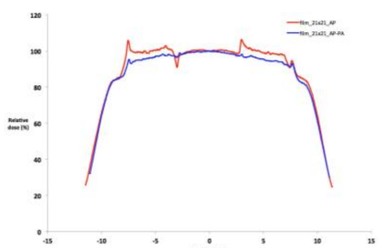

Heterogeneity IC measurements

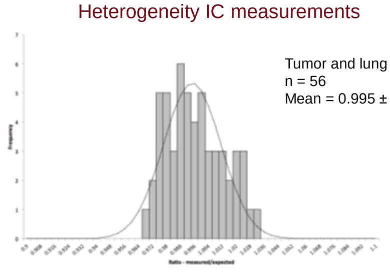

Tumor and lung IC points
n = 56
Mean = 0.995 ± 0.016

Limitation of experimental dosimetry

- Quantitative water-equivalent dosimeters limited
- Setup and calibration errors
- Hybrid approach: a computational system to complement the experimental approach
  Adding another layer of confidence
- Only Monte-Carlo method capable of dealing with radiation transport in a magnetic field

gPENELOPE

A GPU-accelerated Monte Carlo dose calculation platform and its application toward validating an MRI-guided radiation therapy beam model

Yuhe Wang, Thomas R. Mazur, Olga Green, Yanle Hu, Hua Li, Vivian Rodriguez, H. Omar Wooten, Deshan Yang, Tianyu Zhao, Sasa Mutic, and H. Harold Li[a)]

- ❑ PENELOPE (Penetration and ENErgy LOss of Positrons and Electrons): a general-purpose, accurate open source Monte-Carlo engine
- ❑ Original code slow and not support multithreading
- ❑ Translated PENELOPE from FORTRAN to C++ and validated that the translation produced equivalent results
- ❑ Adapted the C++ code to CUDA in a workflow optimized for GPU architecture
- ❑ Expanded upon the original code to include voxelized transport in a magnetic field
- ❑ Incorporated the vendor-provided MRIdian head model into the code
- ❑ Performed a set of experimental measurements to examine the accuracy of both the head model and gPENELOPE

gPENELOPE DoseViewer

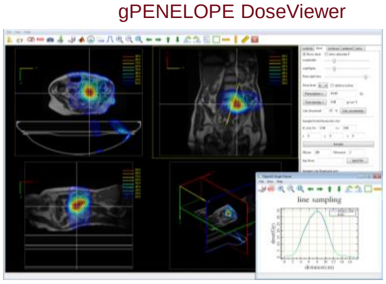

PDD and off-axis profiles

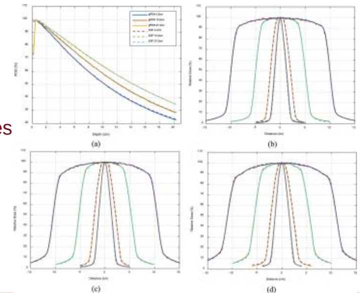

Output factors

Table II. Output factor comparison for square and rectangular fields.

Field shape	Size (cm^2)	OF (gPEN)	OF (expt.)	Diff. (%)
Square field	4.2 × 4.2	0.8839	0.8780	0.67
	6.3 × 6.3	0.9414	0.9380	0.36
	10.5 × 10.5	1.0000	1.0000	NA
	14.7 × 14.7	1.0293	1.0410	−1.12
	27.3 × 27.3	1.0624	1.0700	−0.71
Rectangular field	0.6 × 10.5	0.2103	0.2070	1.58
	0.8 × 10.5	0.2839	0.2825	0.51
	1.0 × 10.5	0.3607	0.3568	1.08
	1.5 × 10.5	0.5256	0.5246	0.19
	2.0 × 10.5	0.6741	0.6721	0.30
	2.5 × 10.5	0.7953	0.7859	1.19
	3.0 × 10.5	0.8730	0.8583	1.71
	4.0 × 10.5	0.9222	0.9119	1.13
	6.0 × 10.5	0.9636	0.9582	0.56
	8.0 × 10.5	0.9837	0.9822	0.16
	10.5 × 10.5	1.0000	1.0000	NA

Point dose comparisons

Table III. TG-119 point dose comparisons: gPENELOPE vs IC.

TG-119 plans	Location	IC (Gy)	gPENELOPE (Gy)	Diff. (%)
AP-PA	Isocenter	1.988	1.991	0.16
Bands	Isocenter	1.422	1.426	0.31
Multitarget	Isocenter	2.085	2.058	−1.29
Multitarget	4 cm superior	1.062	1.038	−2.22
Multitarget	4 cm inferior	0.621	0.593	−4.43
C-shape	2.5 cm anterior	2.152	2.131	−0.96
C-shape	1 cm posterior	0.917	0.882	−3.77
Head and neck	Isocenter	2.215	2.265	2.26
Head and neck	5 cm posterior	0.917	0.919	0.27
Prostate	Isocenter	1.817	1.85	1.82
Prostate	4.5 cm posterior	0.372	0.374	0.62

2D film measurements

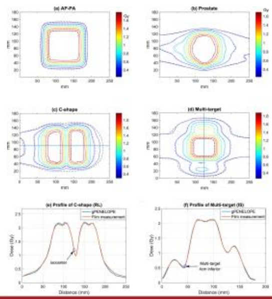

Washington University School of Medicine in St. Louis

Department of Radiation Oncology
Medical Physics Division

Gamma and z-score comparisons

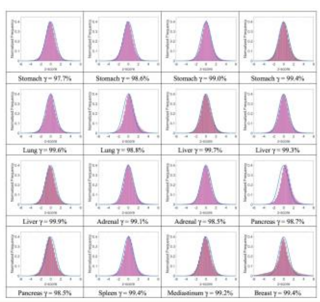

Washington University School of Medicine in St. Louis

Department of Radiation Oncology
Medical Physics Division

MLC performance

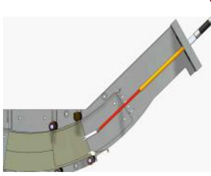

Single stack/ double focused for cobalt

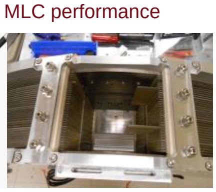

Double stack/double focused for Linac

- Leaf transmission
- Tongue and groove
- Positioning accuracy
- Leaf speed
- Leaf penumbra
- Output factor
- Reproducibility
- Modeling

Performance of a multi leaf collimator system for MR-guided radiation therapy

Bin Cai,[a)] Harold Li, Deshan Yang, Vivian Rodriguez, Austen Curcuru, and Yuhe Wang
Department of Radiation Oncology, Washington University, St. Louis, MO 63110, USA

Washington University School of Medicine in St. Louis

Department of Radiation Oncology
Medical Physics Division

Gated MRgIMRT

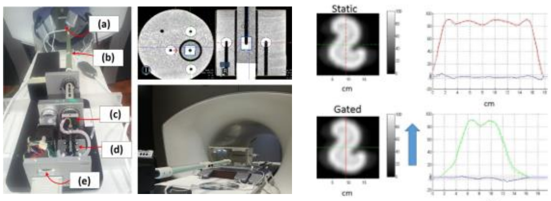

First clinical implementation of real-time, real anatomy tracking and radiation beam control

Olga L. Green[a]
Washington University School of Medicine, St. Louis, MO 63110, USA

MRI-LINAC

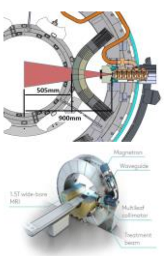

- Radiation field characterization
- Radiation transport in a magnetic field
- Monte Carlo dose calculation
- Dosimeter development
- Online adaptive IMRT optimization
- Real-time dosimetry QA
- Dose accumulation: QUANTAC

The NEW ENGLAND JOURNAL of MEDICINE

ORIGINAL ARTICLE

Noninvasive Cardiac Radiation for Ablation of Ventricular Tachycardia

Phillip S. Cuculich, M.D., Matthew R. Schill, M.D., Rojano Kashani, Ph.D., Sasa Mutic, Ph.D., Adam Lang, M.D., Daniel Cooper, M.D., Mitchell Faddis, M.D., Ph.D., Marye Gleva, M.D., Amit Noheria, M.B., B.S., Timothy W. Smith, M.D., D.Phil., Dennis Hallahan, M.D., Yoram Rudy, Ph.D., and Clifford G. Robinson, M.D.

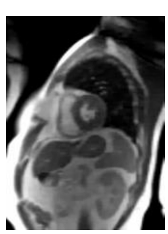

The New York Times

A 'Game Changer' for Patients With Irregular Heart Rhythm

Acknowledgment

- Wash U MRgRT Team
- Yuhe Wang
- Leith Rankine
- Omar Wooten
- Mark Oldham, Duke

SITEMAN CANCER CENTER

BARNES JEWISH Hospital BJC HealthCare | Washington University in St. Louis School of Medicine